Apoptosis (2023) 28:362–378
https://doi.org/10.1007/s10495-022-01787-0

Adipose mesenchymal stem cells-derived exosomes alleviate osteoarthritis by transporting microRNA -376c-3p and targeting the WNT-beta-catenin signaling axis

Feng Li[1] · Zhiming Xu[1] · Zheng Xie[1] · Xing Sun[1] · Chengxiang Li[1] · Yangyang Chen[1] · Jianzhong Xu[1] · Guofu Pi[1]

Accepted: 19 October 2022 / Published online: 17 November 2022

Abstract

Osteoarthritis (OA), one of the major diseases afflicting the elderly, is a type of degenerative joint disease related to cartilage and synovium. This study aimed to clarify the role and mechanism of adipose mesenchymal stem cell (ADSC)-derived exosomes (Exos) in OA-induced chondrocyte degradation and synovial hyperplasia, thus improving the quality of life of patients. The rat OA model, chondrocytes, synovial fibroblast models and immunofluorescence were applied to observe the in vivo and in vitro functions of human ADSC (hADSC)-derived Exos in OA and its possible regulatory signaling pathways. Bioinformatics software and luciferase reporter assay were carried out to verify the mechanism of microRNA-376c-3p (miR-376c-3p) in hADSC-derived Exos in OA in vitro. Moreover, Safranine O-Fast Green Cartilage staining, Masson staining, immunohistochemistry and immunofluorescence were conducted to verify the role of miR-376c-3p in hADSC-derived Exos in OA in vivo. hADSC-derived Exos mitigated OA-induced chondrocyte degradation and synovial fibrosis both in vivo and in vitro models by repressing the WNT-beta-catenin signaling pathway. For the mechanism exploration in vitro, miR-376c-3p was raised in hADSC-derived Exos and mediated the fibrosis of synovial fibroblasts in OA, and miR-376c-3p targeted the 3'-untranslated region of WNT3 or WNT9a. Meanwhile, the in vivo experiments also corroborated that the miR-376c-3p in hADSC-derived Exos mitigated OA-induced chondrocyte degradation and synovial fibrosis. MiR-376c-3p in hADSC-derived Exos repressed the WNT-beta-catenin pathway by targeting WNT3 or WNT9a, and then mitigating OA-induced chondrocyte degradation and synovial fibrosis, thereby providing theoretical basis for clinical implementation of treatment.

Keywords Adipose mesenchymal stem cells · Exosome · miR-376c-3p · WNT-beta-catenin · Osteoarthritis

Abbreviations

OA	Osteoarthritis
ADSC	Adipose mesenchymal stem cell
Exos	Exosomes
hADSC	Human ADSC
ECM	Extracellular matrix
MSCs	Mesenchymal stem cells
MIA	Monosodium iodoacetate
PBS	Phosphate buffer saline
LPS	Lipopolysaccharide
IHC	Immunohistochemistry
EdU	5-Ethynyl-2-deoxyuridine
HPF	High-power field
CT	Cycle threshold
SDS-PAGE	Sulfate-polyacrylamide gel electrophoresis
PVDF	Polyvinylidene fluoride
3′UTR	3′-Untranslated region
miRNAs	MicroRNAs
SO	Safranine O-fast green cartilage
NC	Negative control

✉ Feng Li
Fengli_jea@163.com

✉ Jianzhong Xu
Jianzhong_xu7@163.com

✉ Guofu Pi
Guofu_Pi@126.com

[1] Department of Orthopedics, The First Affiliated Hospital of Zhengzhou University, No. 1, Jianshe East Road, Zhengzhou 450052, Henan, People's Republic of China

Introduction

Osteoarthritis (OA) is a common degenerative joint disease involving cartilage and synovium and is a key factor leading to pain and disability [1, 2]. OA is the result of various cell

interactions, among which chondrocytes and synovial fibroblasts are bound up with OA progression [3, 4]. Increasing studies confirm that the destruction of articular cartilage in OA is mainly caused by the imbalance between the synthesis and degradation of the cartilage extracellular matrix (ECM). Among them, the metalloproteinases secreted by chondrocytes, such as MMP13 and proteoglycanases (aggrecanases, ADAMTS-4/5), induce the degradation of chondrocytes [5, 6]. Synovium is a thin membranous tissue that surrounds the joints and secretes compounds such as hyaluronic acid and lubricant to maintain normal joint function, and synovial fibrosis triggers OA by aggravating joint dysfunction [7]. Synovial fibroblasts are affected by the intra-articular microenvironment to generate inflammatory factors and induce synovitis, leading to synovial hyperplasia and even fibrotic lesions, which directly raise the burden of OA patients [8, 9]. Therefore, restraining cartilage degradation and reducing synovial hyperplasia have the potential to relieve OA.

Mesenchymal stem cells (MSCs) are a momentous member of the stem cell family and have cartilage regeneration functions [10, 11]. Previous studies expound that adipose mesenchymal stem cells (ADSCs) can be applied as seed cells for the repair of OA cartilage injury, thereby delaying OA development [12, 13], 14]. However, the direct application of MSCs to treat OA has certain limitations, mainly including the potential for immune rejection [15]. Thus, probing into a novel method that can take full advantage of MSC therapy and reduce potential risks is conducive to mitigate OA. As we all know, exosomes (Exos) are membrane-bound vesicles secreted by cells and mediate communication between different cells [16, 17]. Importantly, compared with other stem cell-derived Exos, MSC-derived Exos have higher stability and lower immunogenicity under different physiological and pathological conditions [18, 19]. Emerging evidence expounds that MSC-derived Exos play pivotal functions in cartilage regeneration and OA treatment [20]. Because hADSCs produce and secrete more Exos than MSCs, and these Exos inherit a variety of cellular functions. Thus, hADSC-derived Exos are more versatile than MSC-derived Exos [21]. To our knowledge, hADSC-derived Exos function in OA have not been studied. Therefore, this study aimed to firstly probe into the role and mechanism of hADSC-derived Exos in OA-induced chondrocyte degradation and synovial hyperplasia.

In the present study, we applied monosodium iodoacetate (MIA)-induced rat OA model, IL-1β-induced chondrocytes, and IL-1β or TGF-β1-induced synovial fibroblast models to probe into the potential mechanism of hADSC-derived Exos in OA-induced chondrocyte degradation and synovial hyperplasia.

Materials and methods

Isolation and identification of hADSCs

We collected subcutaneous thigh adipose tissues of patients who underwent liposuction operation at the Plastic Surgery Department of the First Affiliated Hospital of Zhengzhou University from November 2018 to April 2019. This study was approved by the Institute Research Medical Ethics Committee of the First Affiliated Hospital of Zhengzhou University. Written informed consents were obtained from all the patients involved. A total of 20 g adipose tissues was washed twice in a sterile environment, treated with 0.1% collagenase type I for approximately 45 min, centrifuged at 800 r/min at room temperature for about 5 min, and resuspended and centrifuged twice. The cell suspension was plated in a 75 cm^2 culture flask, labeled as the P0 generation. P0 cells were incubated at 37 °C, 5% CO_2 environment. When the P0 cells grew to 80% ~ 90%, they were passaged in a certain proportion. The P3 generation was applied in this study. The flow cytometry (FACSCanto II; BD Biosciences, San Jose, CA, USA) was conducted to identify the hADSCs [22]. The anti-CD45 (ab10559, 1:100), anti-D29 (ab134179, 1:100), anti-CD31 (ab134168, 1:100), and anti-CD90 (ab23894, 1 μg) antibodies were obtained from Abcam (Cambridge, UK).

Induction of osteogenesis and adipogenesis of hADSCs

When the P3 generation hADSCs grew to 80–90%, their culture medium was replaced with osteogenic induction solution (dexamethasone sodium phosphate 10^{-8} mol/l, ascorbic acid 0.1 mmol/l, and DMEM/F12 medium, all from Gibco, Waltham, MA, USA) [23]. The supernatant was discarded after 21 days of culture. The cells were fixed with 4% paraformaldehyde solution for nearly 5 min and stained with alizarin red staining solution (Gibco, Waltham, MA, USA) for 20 min. Then the cells were observed under an inverted phase-contrast microscope (Olympus, Tokyo, Japan). For the induction of adipogenesis, the hADSC adipogenic differentiation medium was obtained from Cyagen (HUXMD-90031, Suzhou, Jiangsu, China), and was used given the manufactures' instructions. The cells were fixed with 4% paraformaldehyde solution for 5 min and stained with Oil Red O staining solution (Roche, Basel, Switzerland) for nearly 10 min. Subsequently, the cells were observed under an inverted phase-contrast microscope (Olympus, Tokyo, Japan).

Isolation and identification of hADSC-derived Exos

The hADSC supernatant was centrifuged at 2000 g at 4 °C for 30 min, and the precipitate was discarded. Then the sample was centrifuged at 20,000×*g* at 4 °C for nearly 1 h, followed by discarding the precipitate and repeating the centrifugation. After that, the supernatant was centrifuged at 100,000×*g* at 4 °C for 1 h, followed by discarding the supernatant and repeating the centrifugation once after washing with phosphate buffer saline (PBS) [24]. After being resuspended with 200 µl PBS after discarding the supernatant, the collected precipitate was the hADSC-derived Exos. The isolated Exos (10 µl) were dropped on a 300-mesh copper net and stained with 3% phosphotungstic acid solution for 1 min, dried and observed with a transmission electron microscope (HT7830, HITACHI, Ltd., Tokyo, Japan). The expressions of Exo markers, containing CD63 (ab59479, 1:500, Abcam), TSG101 (ab125011, 1:1000, Abcam), and CD9 (ab92726, 1:2000, Abcam) were determined using Western blot.

Establishment of the rat OA model

All animal experiments were complied with the ARRIVE guidelines and were carried out following the U.S. Public Health Service Policy on Humane Care and Use of Laboratory Animals. SD rats weighing from 230 to 280 g were obtained from the Shanghai Lab Animal Research Center (Shanghai, China). To establish the osteoarthritis model, 50 µl monosodium iodoacetate (MIA, 3 mg in saline) was injected into the right knee joint of the rats [25]. The control rats (Sham group) were injected with the same volume of saline. After 2 weeks of MIA injection, Exos (100 µg/250 µl) were injected into the right knee joint of the rats as the OA + exosome group [26]. There were five rats in each group. The rats were sacrificed 2 weeks later and the knee joint tissues were gathered for subsequent testing.

To investigate the therapeutic effects of exosomal microRNA-376c-3p (miR-376c-3p), the miR-376c-3p antagomir (RiboBio Technology, Guangzhou, Guangdong, China) was injected into the right knee joint of OA rats together with Exos. The control antagomir (anta NC) was applied as the negative control (NC). Two weeks after the establishment of the rat OA model, 50 nmol anta NC (OA + anta NC group), 100 µg Exos and 50 nmol anta-NC (OA + Exo + anta NC group) or 100 µg Exos and 50 nmol miR-376c-3p antagomir (OA + Exo + miR anta group) were injected into the right knee joint of the rats. There were five rats in each group. The rats were sacrificed 2 weeks later, and the knee joint tissues were gathered for next testing.

Safranine O-fast green cartilage staining and masson staining

The Modified Safranine O-Fast Green FCF Cartilage Stain Kit (G1371, Solarbio Life Sciences, Beijing, China) was applied in the Safranine O-Fast Green FCF Cartilage Staining. Specifically, the isolated knee joint was fixed with 10% formalin for 24 h. After decalcification in 10% (v/v) ETDA, the sections were embedded in paraffin and made into 5 µm sections. After dewaxing, the sections were stained with the Weigert dye solution for 3–5 min. After the acidic differentiation for 15 s, the sections were washed with distilled water and stained with the fast-green dye solution for about 5 min. Before being stained with safranine O dye solution for 5 min, the sections were washed with the weak acid solution for 10–15 s. The Masson's Trichrome Stain Kit (G1340, Solarbio Life Sciences, Beijing, China) was applied in the Masson staining. The staining procedure was performed given the manufactures' instructions. Then the sections were dehydrated and observed under an inverted phase-contrast microscope (Olympus, Tokyo, Japan).

Cell culture and treatment

Human chondrocytes were bought from Procell Technology (CP-H096, Wuhan, Hubei, China). The chondrocytes were put in the human articular chondrocyte complete medium (CM-H096, Procell Technology) at 37 °C. Chondrocytes were treated with IL-1β (10 ng/ml) for about 24 h to induce the chondrocyte injury and they were treated with Exos (10 µg/ml) to relieve the IL-1β-induced injury.

The isolation and culture of rat primary synovial fibroblasts were carried out given the previously described method with minor changes [27]. In brief, the rat synovial tissues were digested with enzymes trypsin and collagenase and filtered using sterile 20 µm sieve to separate synovial fibroblasts. The synovial fibroblasts were put in DMEM and 10% fetal bovine serum (FBS, Solarbio Life Sciences, Beijing, China) until a fusion of nearly 80% was achieved. The rat primary synovial fibroblasts were treated with IL-1β (10 ng/ml) or lipopolysaccharide (LPS, 50 ng/ml) for nearly 24 h to induce the inflammatory responses and they were treated with Exos (10 µg/ml) to relieve such responses.

In order to verify the role of miR-376c-3p on WNT3, WNT9a and β-catenin expreesions, miR-376c-3p inhibitior (RiboBio Technology) was transfected into chondrocytes or synovial fibroblasts. To further search for whether miRNAs in Exos functioned in OA progression, we treated the chondrocytes and synovial fibroblasts with hADSC-derived Exos,and then continued to treat the cells with 100 µg/ml RNase for about 1 h at 37 °C [28].

Immunohistochemistry and immunofluorescence staining

Collagen II expression in rat cartilage tissues was determined using immunohistochemistry (IHC) [29]. The anti-Collagen II antibody (ab34712, Abcam) was applied during the IHC. The percentage of Collagen II positive cells per high-power field (HPF) was calculated by randomly selecting 4 HPFs. For the immunofluorescence staining, human chondrocytes were incubated with the anti-Collagen II antibody (ab34712, Abcam) or anti-MMP13 antibody (ab39012, Abcam) after penetrating cell membrane using 0.5% Triton X-100, followed by the incubation with the second antibody conjugated with fluorescence for nearly 1 h [30]. The rat primary synovial fibroblasts were incubated with anti-Collagen III antibody (ab7778, Abcam) or anti-α-SMA antibody (ab32575, Abcam) for immunofluorescence staining. The rat cartilage tissues and the rat synovial tissues were incubated with anti-β-catenin antibody (ab16051, Abcam) for immunofluorescence staining.

Cell proliferation assay

The cell proliferation of synovial fibroblasts was tested using the 5-Ethynyl-2-deoxyuridine (EdU) labeling detection [31]. The synovial fibroblasts were exposed to 50 μM EdU (RiboBio, Guangzhou, China). Subsequently, the contents were stained with DAPI (Thermo Fisher Scientific) for approximately 30 min and visualized under microscopy (Olympus, Tokyo, Japan).

Quantitative real-time PCR (qRT-PCR)

Given the previously described method [32], we carried out the qRT-PCR assay. Specifically, the TRIzol lysate (Thermo Fisher Scientific) was conducted to extract the total RNA. The PrimeScript™RT reagent Kit (RR047AA, Takara, Dalian, Liaoning, China) was applied during the reverse transcription after determining the RNA concentration. The PCR reaction systems were presented: 95 °C (5 min); 40 cycles of 95 °C (30 s), 60 °C (30 s), 72 °C (1 min); 72 °C (10 min). U6 was the internal control of miR-376c-3p, and GAPDH was the internal control of mRNAs. Cycle threshold (CT) values were calculated by $2^{-\Delta\Delta CT}$ to quantify the relative gene expressions.

Western blot analysis

RIPA buffer (Gibco, Waltham, MA, USA) was applied to isolate total proteins. The proteins were quantified using a BCA Protein Assay Kit (Thermo Fisher Scientific). After performing the sodium dodecyl sulfate–polyacrylamide gel electrophoresis (SDS-PAGE) for about 2.5 h, the samples were transferred to the polyvinylidene fluoride (PVDF) membranes (Sigma-Aldrich, St Louis, MO, USA). After being blocked using 3% bovine serum albumin (BSA, Thermo Fisher Scientific), the samples were incubated with primary antibodies, containing MMP13 (ab39012, 1:3000, Abcam), ADAMTS5 (ab41037, 1:250, Abcam), Collagen II (ab34712, 1:1000, Abcam), Aggrecan (ab3778, 1:100), α-SMA (ab32575, 1:1000, Abcam), Collagen III (ab7778, 1:5000, Abcam), β-catenin (ab16051, 0.25 μg/ml, Abcam), WNT3 (ab32249, 1 μg/ml, Abcam), WNT9a (ab125957, 1 μg/ml, Abcam) and GAPDH (ab8245, 1/500, Abcam), overnight at 4 °C. Then, the samples were incubated with the secondary antibody (ab205718, 1:2000, Abcam) at 37 °C for 1 h. Images were obtained using a Pierce™ ECL Western Blotting Substrate (32,209, Thermo Fisher Scientific).

Luciferase reporter assay

The DNA sequences of the WNT3 3′-untranslated region (3′UTR) and the WNT9a 3′UTR of human (Homo) or rat were amplified by PCR. The sequences were inserted into the pRL-TK-REPORT Vector (Promega, Madison, WI, USA). The 293 T cells (1.2×10^4) in a 96-well plate were co-transfected with 50 nM miR-376c-3p mimic or mimic control (RiboBio Technology, Guangdong, China) and 2 μg/ml WNT3 3′UTR vector or WNT9a 3′UTR vector. After 48 h post-transfection, the luciferase activity was tested using the Luciferase Reporter Assay System (Promega, Madison, WI, USA) and the firefly luciferase activity was normalized to the Renilla luciferase activity [33].

Cell transfection

The miR-376c-3p mimic, obtained from the RiboBio Technology, was carried out to overexpress miR-376c-3p in human chondrocytes and rat primary synovial fibroblasts. The negative control was also from RiboBio Technology. The cell transfection was performed using the Lipofectamine 2000 reagent as previously reported [34].

Endocytosis experiment

The purified Exos were labeled using the green fluorescent PKH67 (Sigma-Aldrich, St Louis, MO, USA) [35]. Briefly, 2 μM PKH67 was added to the hADSC-derived Exos. Then, the labeled Exos were were injected into the right knee joint of the rats. Two weeks later, the knee joint tissues were gathered and the area of cartilage and synovium were observed by fluorescence microscope. The chondrocytes or synovial fibroblasts were co-incubated with the labeled Exos for 24 h. After that, the cell supernatant was discarded and the percentage of PKH67 positive cells was tested using the flow

cytometry (FACSCanto II; BD Biosciences, San Jose, CA, USA).

Statistical analysis

All cell experiments had at least three independent biological replicates for quantitative analysis. Data were presented as mean ± standard deviation. We applied the Graphpad Prism 5.0 and the SPSS 18.0 (IBM, Armonk, NY, USA) to assess data. The difference between the two groups was compared using the unpaired two-tailed Student's *t*-test. The difference among multiple groups was compared using the one-way ANOVA analysis combined with Games-Howell Post-Hoc or LSD post hoc test, Kruskal-Wallis test with Dunn's post-hoc. When $P < 0.05$, the differences were considered statistically significant.

Results

Exosomes derived from hADSCs mitigate OA in SD rats

Here, we first probed into whether the hADSC-derived Exos functioned in OA. The identification of hADSC-derived Exos and the identification of Exos entering chondrocytes and synovial fibroblasts were displayed in Supplementary Fig. 1. After establishing a rat model of OA, hADSC-derived Exos were injected into the rats, the specific protocols were displayed in Fig. 1A. Safranine O-fast green cartilage (SO) Staining expounded that the cartilage tissue degradation in the OA group was severe, while this effect was relieved after hADSC-derived Exos injection. Masson staining analysis authenticated that the fibrosis in the OA group was aggravated, while hADSC-derived Exos injection reduced the fibrosis (Fig. 1B). The Osteoarthritis research society international (OARSI) evaluation in the OA group displayed a higher score than the sham group, while hADSC-derived Exos injection reduced the OARSI score (Fig. 1B). The above data authenticated that hADSC-derived Exos had the function of mitigating OA in SD rats.

hADSC-derived Exos promote the expression of Collage II in cartilage tissues

Next, we investigated the potential mechanism of hADSC-derived Exos to mitigate OA. Immunohistochemical staining of Collagen II on the cartilage tissues expounded that Collagen II was lessened in the OA group, and the injection of hADSC-derived Exos increased Collagen II (Fig. 2A). Besides, as displayed in Fig. 2B, after injection of hADSC-derived Exos, the expressions of inflammatory factors (IL-1β, iNOS, TNF-α, IL-6 and IFN-γ), chondroprotection-related molecules (Col2a1, Sox9, Comp and ACAN) and fibrosis-related molecules (α-SMA, Col1a3, MMP3, MMP13, TIMP1, TIMP2, ADAMTS4 and ADAMTS5) changed memorably and the pain and proliferation-related molecules (CGRP, NGF, P75NTR, PCNA, Bax, casp3 and casp8) had no remarkable changes. Thus, we selected these indicators for subsequent detection.

hADSC-derived Exos mitigate the dysfunction of chondrocytes induced by IL-1β and synovial fibroblasts induced by IL-1β or TGF-β1

We next explored the hADSC-derived Exos functions in chondrocytes and synovial fibroblasts. As displayed in Fig. 3A, IL-1β treatment lessened Collage II and raised MMP13, while these trends were partly reversed after the hADSC-derived Exos treatment. Western blot analysis expounded that IL-1β treatment enhanced extracellular matrix related molecules MMP13 and ADAMTS5 expressions, and weakened chondrocyte marker molecule Collagen II and Aggrecan expressions, while these effects were partly reversed after the hADSC-derived Exos treatment, prompting that hADSC-derived Exos restrained chondrocyte degradation (Fig. 3B). Furthermore, IL-1β treatment raised inflammatory cytokines TNF-α and IL-6 in synovial fibroblasts, while this raise was partly reversed after the hADSC-derived Exos treatment (Fig. 3C). The LPS treatment enhanced inflammatory cytokines IL-1β, IL-6, TNF-α and IFN-γ expressions in synovial fibroblasts, while this enhance was reversed after the hADSC-derived Exos treatment, hinting that hADSC-derived Exos mitigated the inflammatory response of synovial fibroblasts (Fig. 3D). Moreover, TGF-β1 treatment raised fibrosis-related molecules α-SMA and Collagen III in synovial fibroblasts, and this raise was reversed after the hADSC-derived Exos treatment (Fig. 3E). Besides, in the synovial fibroblasts of OA rats, we also corroborated that hADSC-derived Exos treatment reduced the induction effect of TGF-β1 on the synovial fibroblasts (Supplementary Fig. 2). Meanwhile, as displayed in Fig. 3F, the trends of α-SMA and Collagen III expressions in synovial fibroblasts detected by immunofluorescence were the same as that in Fig. 3E, and the results of EdU cell proliferation authenticated that hADSC-derived Exos restrained the proliferation of synovial fibroblasts induced by TGF-β1 (Fig. 3F). Generally, hADSC-derived Exos restrained IL-1β-induced chondrocyte degradation and mitigated the inflammatory response of synovial fibroblasts induced by IL-1β or LPS, and mitigated the pro-fibrosis and proliferation effects of synovial fibroblasts induced by TGF-β1.

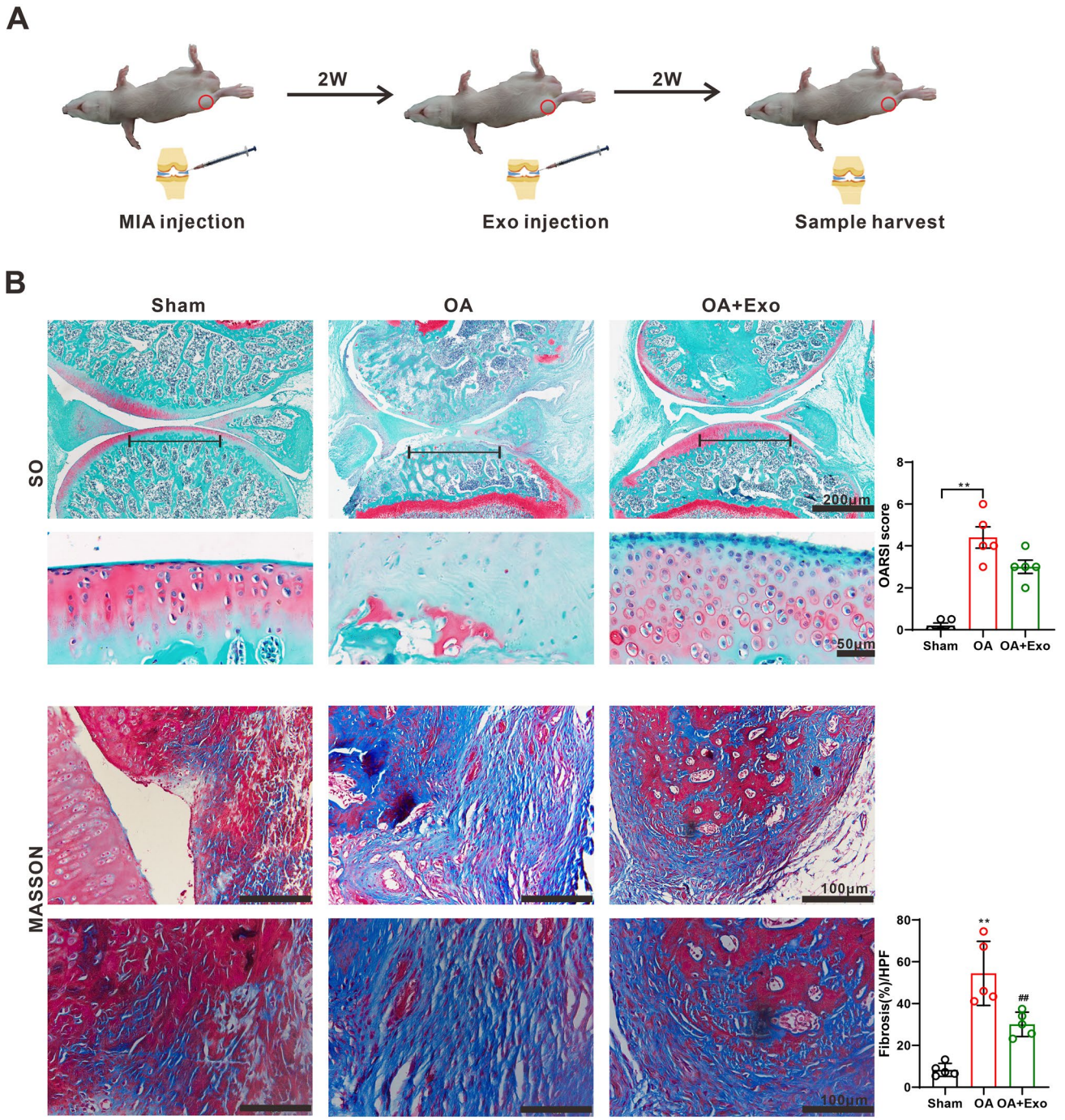

Fig. 1 Effects of adipose mesenchymal stem cells (ADSC)-derived exosomes (Exos) on SD rats with osteoarthritis. **A** The specific protocols for the rat model of osteoarthritis (OA). **B** Safranine O-Fast Green Cartilage (SO) Staining (Scale bar: 200 μm, 50 μm) and Masson staining (Scale bar: 100 μm) were conducted to evaluate the degree of cartilage tissue degradation and synovial fibrosis and the osteoarthritis research society international (OARSI) score was applied. OARSI score: sham vs. OA: Kruskal–Wallis with Dunn's post-hoc, N = 5; OA vs OA + Exo: Kruskal–Wallis with Dunn's post-hoc, N = 5. Fibrosis: One-way ANOVA analysis combined with Tukey's post-hoc, N = 5. $^{**}P < 0.01$ versus. sham, $^{\#\#}P < 0.05$ versus OA. MIA monosodium iodoacetate, SO safranine O-fast green cartilage staining, OA osteoarthritis

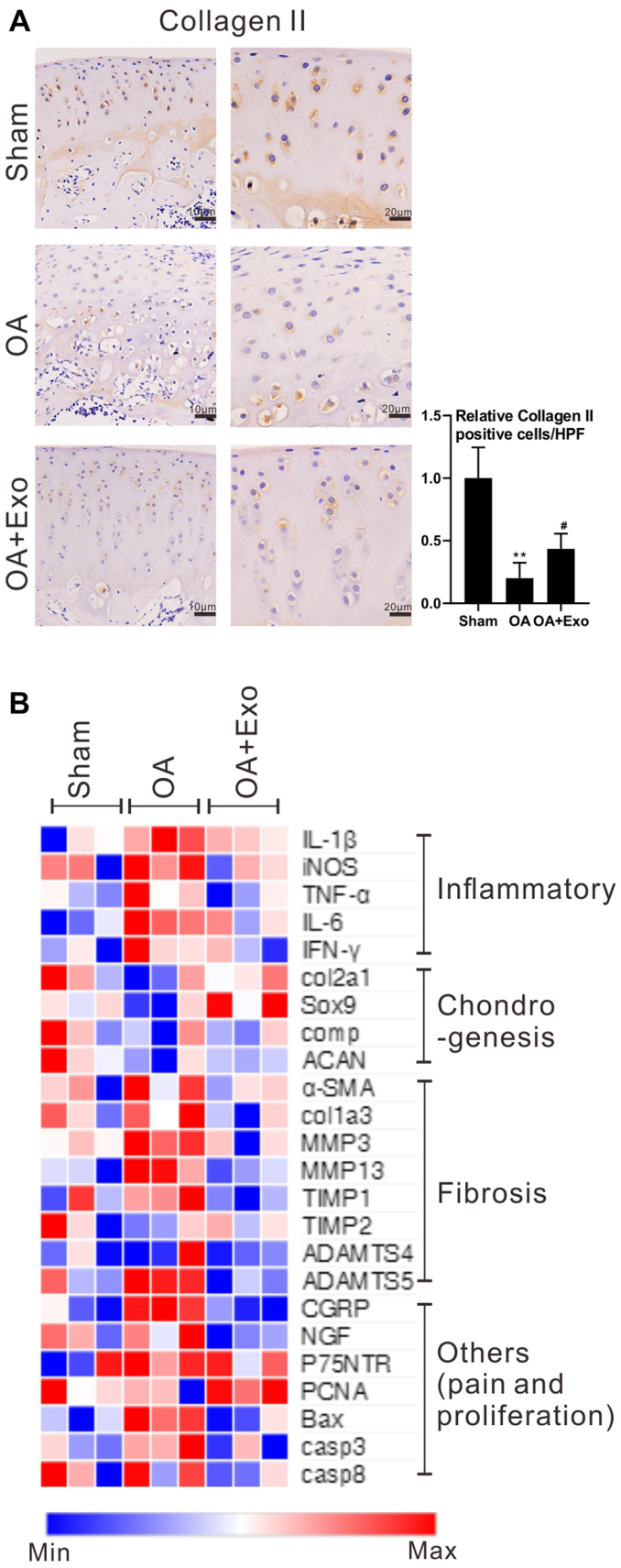

Fig. 2 Effects of hADSC-derived Exos on Collage II in cartilage tissues. **A** Immunohistochemical staining of collagen II on the cartilage tissues (Scale bar: 20 μm). One-way ANOVA analysis combined with Games-Howell Post-Hoc, N = 5. **B** Heat map analysis of inflammatory factors (IL-1β, iNOS, TNF-α, IL-6 and IFN-γ), chondroprotection-related molecules (Col2a1, Sox9, Comp and ACAN) and fibrosis-related molecules (α-SMA, Col1a3, MMP3, MMP13, TIMP1, TIMP2, ADAMTS4 and ADAMTS5) and the pain and proliferation-related molecules (CGRP, NGF, P75NTR, PCNA, Bax, casp3 and casp8). $^{**}P < 0.01$ versus sham, $^{\#}P < 0.05$ versus OA. Exo exosome

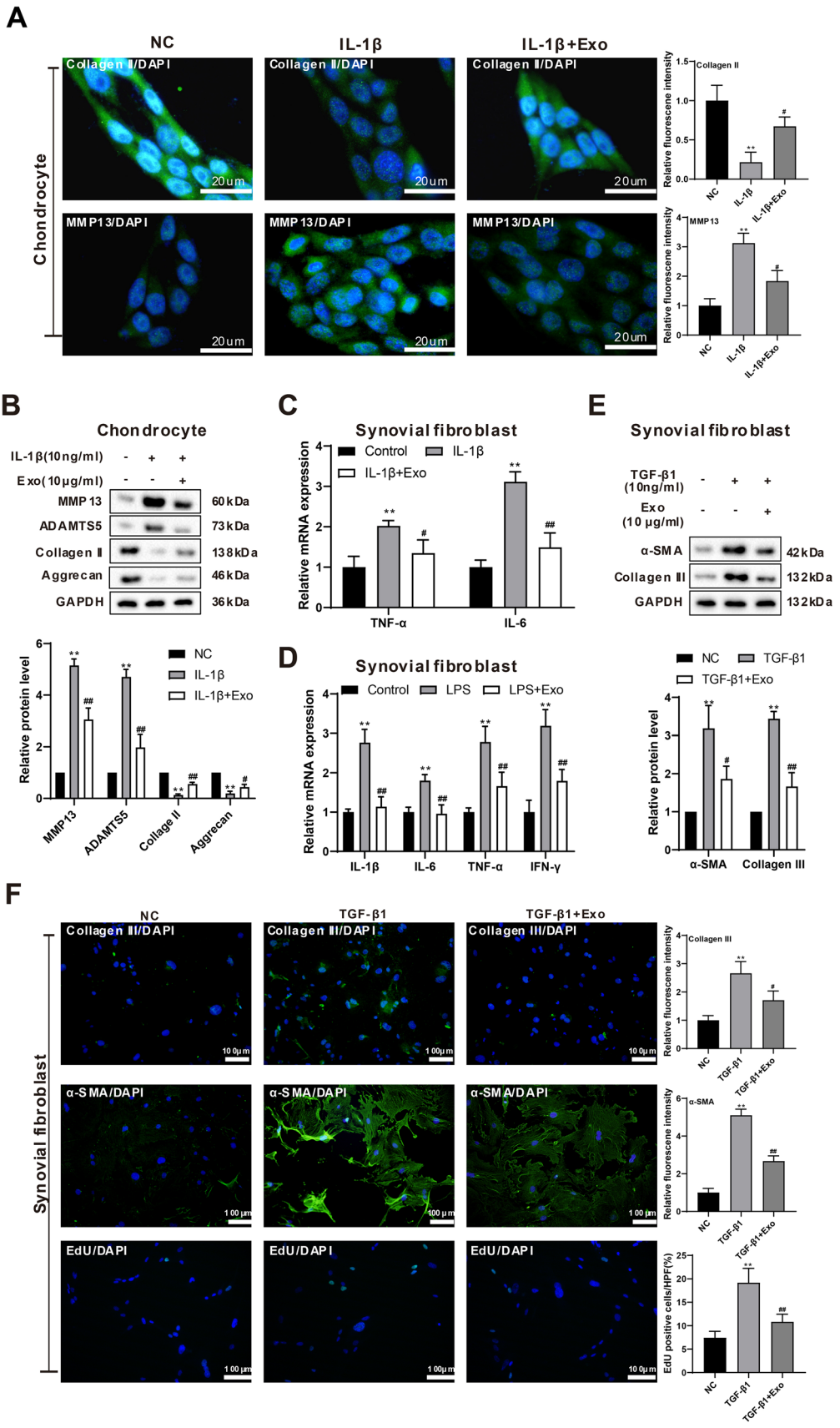
A
NC
IL-1β
IL-1β+Exo
Chondrocyte
Collagen II/DAPI
MMP13/DAPI
20um
Relative fluorescene intensity
Collagen II
MMP13
B
Chondrocyte
IL-1β(10ng/ml)
Exo(10μg/ml)
MMP 13
ADAMTS5
Collagen II
Aggrecan
GAPDH
60kDa
73kDa
138kDa
46kDa
36kDa
Relative protein level
MMP13
ADAMTS5
Collage II
Aggrecan
C
Synovial fibroblast
Control
IL-1β
IL-1β+Exo
Relative mRNA expression
TNF-α
IL-6
D
Synovial fibroblast
Control
LPS
LPS+Exo
IL-1β
IL-6
TNF-α
IFN-γ
E
Synovial fibroblast
TGF-β1 (10ng/ml)
Exo (10 μg/ml)
α-SMA
Collagen III
GAPDH
42kDa
132kDa
132kDa
NC
TGF-β1
TGF-β1+Exo
α-SMA
Collagen III
F
NC
TGF-β1
TGF-β1+Exo
Synovial fibroblast
Collagen III/DAPI
α-SMA/DAPI
EdU/DAPI
100μm
Relative fluorescene intensity
EdU positive cells/HPF(%)

◂**Fig. 3** Effect of hADSC-derived Exos on the chondrocytes induced by IL-1β and synovial fibroblasts induced by IL-1β or TGF-β1. 10 ng/ml IL-1β alone or 10 ng/ml IL-1β combined with 10 ug/ml hADSC-derived Exos were carried out to treat human chondrocytes CP-H096 for nearly 24 h. **A** Immunofluorescence detection of Collage II and MMP13 (Scale bar: 20 μm). One-way ANOVA analysis combined with LSD post-hoc, N = 3. **B** Western blot detection of MMP13, ADAMTS5, Collagen II and Aggrecan. 10 ng/ml IL-1β alone or 10 ng/ml IL-1β combined with 10 ug/ml hADSC-derived Exos were applied to treat synovial fibroblasts for about 24 h. Unpaired two-tailed Student's t-test, N = 3. **C** Detection of TNF-α and IL-6 expressions by qRT-PCR. 50 ng/ml LPS alone or 50 ng/ml LPS combined with 10 ug/ml hADSC-derived Exos were conducted to treat synovial fibroblasts for nearly 24 h. One-way ANOVA analysis combined with LSD post-hoc, N = 3. **D** Detection of IL-1β, IL-6, TNF-α, and IFN-γ expressions using qRT-PCR. 10 ng/ml TGF-β1 alone or 10 ng/ml TGF-β1 combined with 10 ug/ml hADSC-derived Exos were carried out to treat synovial fibroblasts for about 24 h. One-way ANOVA analysis combined with LSD post-hoc, N = 3. **E** Detection of α-SMA and Collagen III protein levels by Western blot. Unpaired two-tailed Student's t-test, N = 3. **F** Immunofluorescence detection of α-SMA and Collagen III (Scale bar: 100 μm), and 5-Ethynyl-2-deoxyuridine (EdU) detection of cell proliferation. One-way ANOVA analysis combined with LSD post-hoc, N = 3. $^{**}P < 0.01$ versus NC or control. $^{\#}P < 0.05$, $^{\#\#}P < 0.01$ versus IL-1β, LPS, and TGF-β1. NC negative control, LPS lipopolysaccharide

hADSC-derived Exos inhibit the WNT-beta-catenin signaling pathway

TO clarify the underlying mechanism behind hADSC-derived Exos mitigating OA in SD rats and restraining the dysfunction of chondrocytes and synovial fibroblasts, we carried out immunofluorescence detection of β-catenin in rat cartilage tissues and rat synovial tissues in vivo, and we mitigate authenticated that β-catenin was raised in the OA group, while β-catenin was lessened in the OA + Exo group (Fig. 4A), and there were more normal chondrocytes in the OA + Exo group than in the OA group (Fig. 4A). The quantitative analysis results were displayed in Fig. 4A. Furthermore, in vitro detection of IL-1β-induced chondrocytes, or LPS or TGF-β1-induced synovial fibroblasts, the expression of β-catenin was enhanced, while β-catenin was lessened after the treatment with hADSC-derived Exos (Fig. 4B), implying that hADSC-derived Exos might mediate the β-catenin signaling pathway. Thus, we further tested the expressions of other important molecules of classical WNT-β-catenin WNT1, WNT2, WNT3, WNT8a, WNT8b, WNT9a, WNT10a and WNT10b. We authenticated that hADSC-derived Exos lessened the mRNA levels of WNT1, WNT2, WNT3 and WNT9a both in synovial fibroblasts and chondrocytes (Fig. 4C and Supplementary Fig. 3A), while RNase treatment raised the protein levels of WNT3 and WNT9a and had no prominent changes in WNT1 and WNT2 protein levels (Fig. 4D and Supplementary Fig. 3B), hinting that the RNA in hADSC-derived Exos might mediate the β-catenin signaling pathway. Considering that we hope to conduct in-depth study on miRNAs carried in hADSC-derived Exos, we chose WNT3 and WNT9a for further studies. In summary, the hADSC-derived Exos restrained the WNT-beta-catenin signaling pathway and the RNA in hADSC-derived Exos might mediate this process.

miR-376c-3p in hADSC-derived Exos regulates chondrocyte and synovial fibroblast function and targets WNT3 or WNT9a

Increasing evidence expound that miRNAs are one of the key molecules that function in Exos [19]. Here, we applied software available online (TargetScan) to computationally identify 19 miRNAs that might target WNT3 and WNT9a gene both in rats and humans, and discovered a total of 11 common miRNAs and the red markers represented the miRNAs whose sequences were conserved both in humans and rats (Supplementary Fig. 4A). miR-376c-3p was highly expressed in hADSC-derived Exos (Supplementary Fig. 4B), which had attracted our attention. Meanwhile, miR-376c-3p expression was raised after chondrocytes and synovial fibroblasts were treated with hADSC-derived Exos (Supplementary Fig. 4C). The expression of mir-376c-3p did not change significantly after chondrocytes or fibroblast was treated with ActD, indicating that the increase in mir-376c-3p expression was not a consequence of endogenous miRNA synthesis, but reflected the direct transfer of Exos. (Supplementary Fig. 4C). Next, we tried to clarify the possible downstream target genes of miR-376c-3p. As displayed in Supplementary Fig. 4D, miR-376c-3p targeted the 3'UTR region of WNT3 or WNT9a, and miR-376c-3p negatively regulated the luciferase activity of WNT3 or WNT9a both in humans and rats. XAV939 is an inhibitor of the WNT-β-catenin signaling pathway [36], and XAV939 treatment was applied as a positive control to prove that miR-376c-3p may function through inactivating the WNT-β-catenin signaling pathway. Furthermore, interference with miR-376C-3p can revised Exo function in chondrocytes and fibroblasts (Supplementary Fig. 4E, F), indicating that miR-376C-3p mediates the regulation of chondrocyte and fibroblast functions by hADSC exosomes in vitro.

Next, as displayed in Fig. 5A, miR-376c-3p overexpression reversed the low Collage II expression and the high MMP13 expression in chondrocytes induced by IL-1β. Also, miR-376c-3p overexpression lessened the protein levels of WNT3, WNT9a and β-catenin in chondrocytes (Fig. 5B). Furthermore, miR-376c-3p overexpression reversed the high expressions of Collagen III and α-SMA in synovial fibroblasts and the high proliferation ability of the cells induced by TGF-β1 (Fig. 5C). Besides, miR-376c-3p overexpression lessened the protein levels of WNT3, WNT9a and β-catenin in synovial fibroblasts (Fig. 5D). In summary, our data authenticated that miR-376c-3p in hADSC-derived Exos

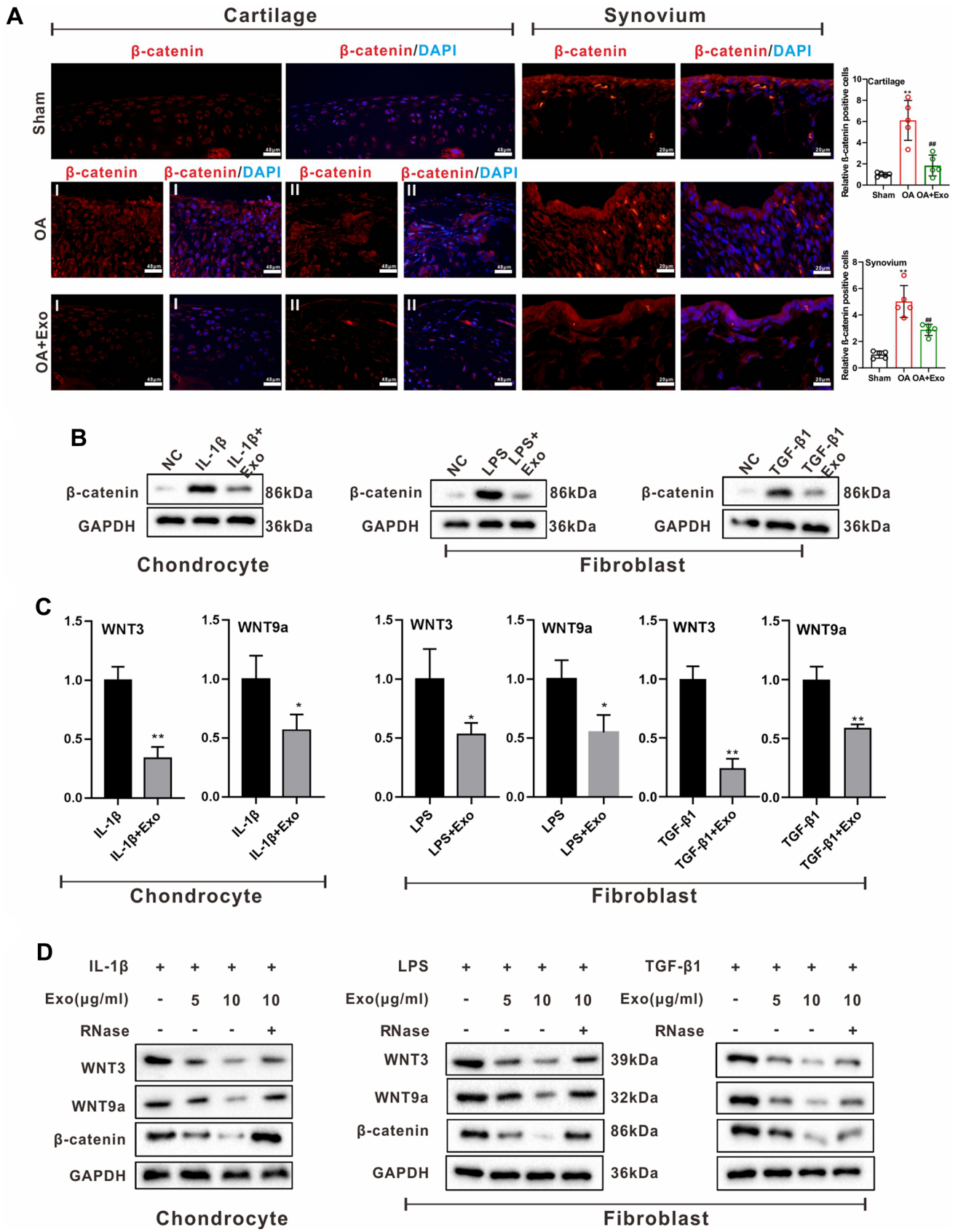
A
Cartilage
Synovium
β-catenin
β-catenin/DAPI
Sham
OA
OA+Exo
Relative β-catenin positive cells
Sham OA OA+Exo
B
NC IL-1β IL-1β+ Exo
β-catenin 86kDa
GAPDH 36kDa
Chondrocyte
NC LPS LPS+ Exo
NC TGF-β1 TGF-β1 Exo
Fibroblast
C
WNT3
WNT9a
IL-1β
IL-1β+Exo
LPS
LPS+Exo
TGF-β1
TGF-β1+Exo
Chondrocyte
Fibroblast
D
IL-1β
LPS
TGF-β1
Exo(μg/ml)
RNase
WNT3 39kDa
WNT9a 32kDa
β-catenin 86kDa
GAPDH 36kDa
Chondrocyte
Fibroblast

◂**Fig. 4** Effect of hADSC-derived Exos on the WNT-beta-catenin signaling pathway. **A** Immunofluorescence detection of β-catenin in rat cartilage tissues and rat synovial tissues in vivo and the quantitative analysis results were presented (Scale bar: 48 μm or 20 μm). One-way ANOVA analysis combined with LSD post-hoc, N = 5. **B** Detection of β-catenin protein level in IL-1β-induced chondrocytes or LPS or TGF-β1-induced synovial fibroblasts by Western blot. **C** Detection of WNT3 and WNT9a mRNA levels in IL-1β-induced chondrocytes or LPS or TGF-β1 induced-synovial fibroblasts by qRT-PCR. The chondrocytes induced by IL-1β or the synovial fibroblasts induced by LPS or TGF-β1 were treated with RNase, respectively. Unpaired two-tailed Student's t-test, N = 3. **D** Detection of WNT3, WNT9a, and β-catenin protein levels by Western blot. $^{*}P < 0.05$ versus IL-1β or LPS. $^{**}P < 0.01$ versus IL-1β, TGF-β1 or sham. $^{\#\#}P < 0.01$ versus OA

regulated the chondrocytes and synovial fibroblasts functions and negatively regulated WNT3 or WNT9a expression.

miR-376c-3p in hADSC-derived Exos participates in the process of hADSC-derived Exos mitigating OA in rats

We then verified miR-376c-3p function in hADSC-derived Exos in the rat OA model in vivo. The specific protocols were displayed in Fig. 6A. The area of cartilage and Synovium presented obvious green fluorescent dots under the fluorescent microscope after intra-articular injection of PKH67-labelled exosomes (Fig. 6A). The SO staining results authenticated that hADSC-derived Exos mitigated the cartilage injury in the rat OA model, and miR-376c-3p antagomir injection aggravated the cartilage injury, hinting that miR-376c-3p mediated the regulation of hADSC-derived Exos on cartilage injury. Masson staining (the synovial fibroblast sites) analysis expounded that hADSC-derived Exos restrained the synovial-hyperplasia and fibrosis, and miR-376c-3p antagomir injection boosted the synovial-hyperplasia and fibrosis, implying that miR-376c-3p mediated the regulation of hADSC-derived Exos on synovial-hyperplasia and fibrosis (Fig. 6B). Overall, miR-376c-3p in hADSC-derived Exos was interrelated to the process of hADSC-derived Exos mitigating OA in rats.

The regulation of miR-376c-3p in hADSC-derived Exos on Collagen II and β-catenin in OA rats

As displayed in Fig. 7A, the hADSC-derived Exos injection raised the Collage II expression, and this raise was reversed after the miR-376c-3p antagomir injection. Immunofluorescence analysis expounded that the hADSC-derived Exos injection lessened the β-catenin expression, and this trend was reversed after the miR-376c-3p antagomir injection (Fig. 7B), and the semi-quantitative statistical results of the above immunohistochemistry and immunofluorescence were displayed in Fig. 7C, D. These data authenticated that miR-376c-3p in hADSC-derived Exos mediated the regulation of hADSC-derived Exos on the Collagen II and β-catenin expressions in OA rats.

Discussion

The focus of this study was to probe into the role and mechanism of hADSC-derived Exos in OA-induced chondrocyte degradation and synovial hyperplasia. Here, we firstly authenticated that hADSC-derived Exos mitigated OA-induced chondrocyte degradation and synovial fibrosis by repressing the WNT-beta-catenin signaling pathway in vivo and in vitro models. Our in-depth mechanism research results expounded that the miR-376c-3p in hADSC-derived Exos authenticated OA-induced chondrocyte degradation and synovial fibrosis by targeting the restraint of WNT3 and WNT9a, and this is the first study to investigate the miR-376c-3p function in hADSC-derived Exos in OA.

Recently, researchers have sought to emphasize the Exos function in the diagnosis and treatment of various human diseases [37]. Due to the large number of Exos produced by MSCs and the immunosuppressive characteristics of MSCs-derived Exos, MSCs-derived Exos gradually attracted extensive attention [38, 39]. Compared with the wide application of Exos derived from other MSCs in OA, there are few studies on hADSC-derived Exos. In the current study, we authenticated that hADSC-derived Exos weakened OA-induced rat cartilage tissue degradation and synovial fibrosis in vivo, and irestrained IL-1β-induced chondrocyte degradation and IL-1β or TGF-β1-induced synovial fibroblast proliferation and fibrosis in vitro. Our results preliminarily authenticated that hADSC-derived Exos lightened OA-induced cartilage tissue degradation and synovial fibrosis.

WNT-beta-catenin signaling pathway plays a momentous role in the OA pathogenesis, and the abnormal activation of this signaling pathway can be found in cartilage tissues and synovial tissues [36, 40]. Recent research expounds that lorecivivint treatment mitigates the symptoms of OA by restraining the WNT pathway and boosting cartilage growth [41]. Besides, the restraint of the WNT-beta-catenin pathway reduces collagen generation and synovial fibroblast proliferation in the OA mouse model, hinting that the WNT-beta-catenin signaling pathway might also regulate OA-induced synovium fibrosis [36]. Here, we authenticated that hADSC-derived Exos mitigated OA-induced chondrocyte degradation and synovial fibrosis by restraining the WNT-beta-catenin signaling axis in vivo and in vitro models, which was consistent with the above researches. Besides, previous studies evaluate the function of the WNT/β-catenin signaling pathway inhibitor SM04690 in clinical trials of OA and preliminarily authenticates that SM04690 is well tolerated [42]. Although the acquisition and preparation of MSCs-derived Exos are relatively complex, MSCs-derived Exos

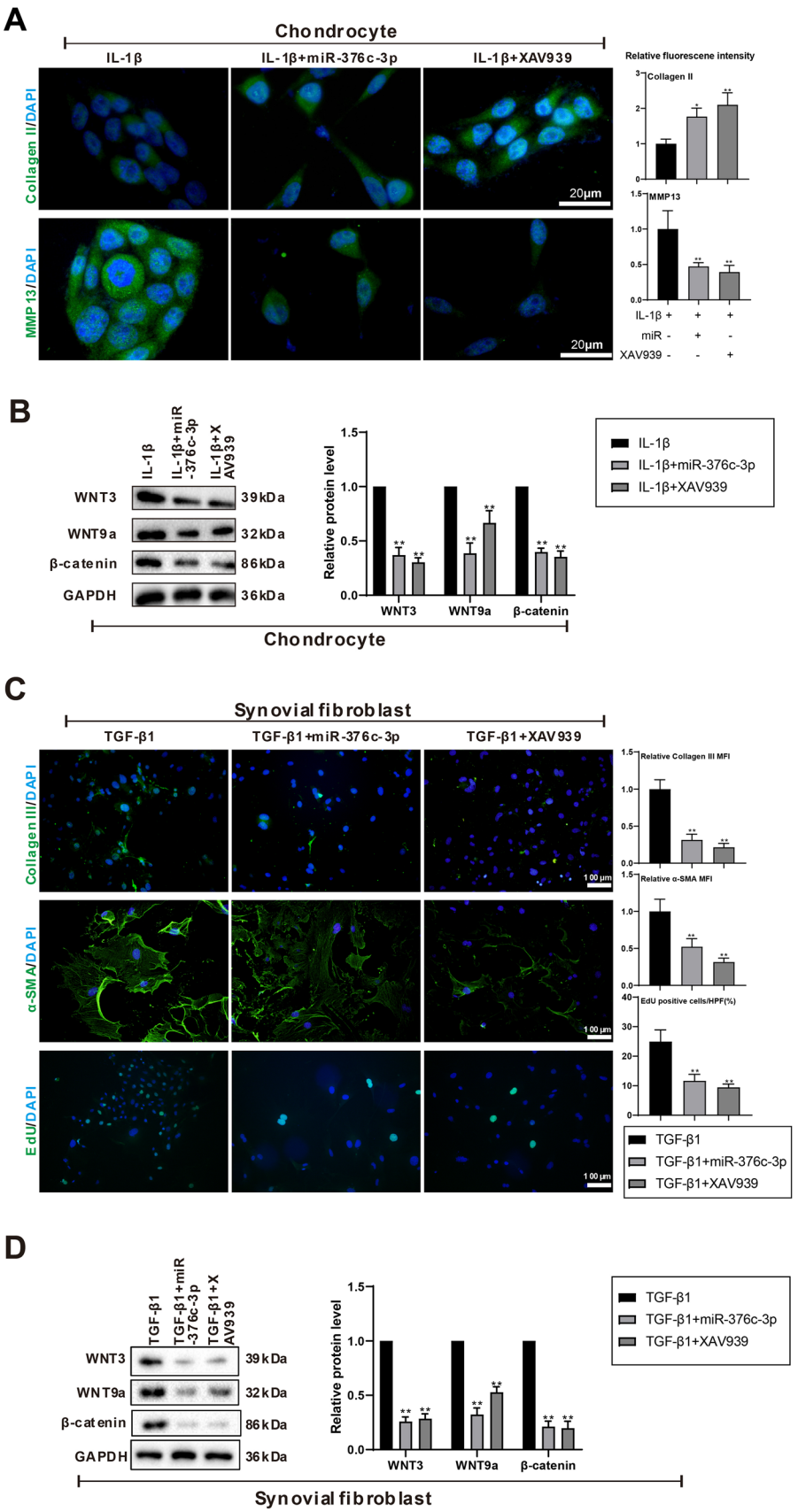

Fig. 5 Effect of miR-376c-3p in hADSC-derived Exos on chondrocytes and synovial fibroblasts and exploration of the interaction between miR-376c-3p and WNT3, miR-376c-3p and WNT9a. **A** miR-376c-3p mimic was transfected into chondrocytes or synovial fibroblasts, and then the cells were treated with IL-1β or TGF-β1, respectively. Detection of Collage II and MMP13 expressions (Scale bar: 20 μm). One-way ANOVA analysis combined with LSD post-hoc, N = 3. **B** Detection of WNT3, WNT9a and β-catenin protein levels in chondrocytes. Unpaired two-tailed Student's t-test, N = 3. **C** Detection of Collage III and MMP13 and cell proliferation (Scale bar: 100 μm). One-way ANOVA analysis combined with LSD post-hoc, N = 3. **D** Detection of WNT3, WNT9a and β-catenin protein levels in synovial fibroblasts. Unpaired two-tailed Student's t-test, N = 3. $^{*}P < 0.05$ versus IL-1β. $^{**}P < 0.01$ versus miR-19a-3p, chondrocyte, fibroblast, control, IL-1β, or TGF-β1. Exo: exosome. XAV939 (WNT-beta-catenin inhibitor): a positive control

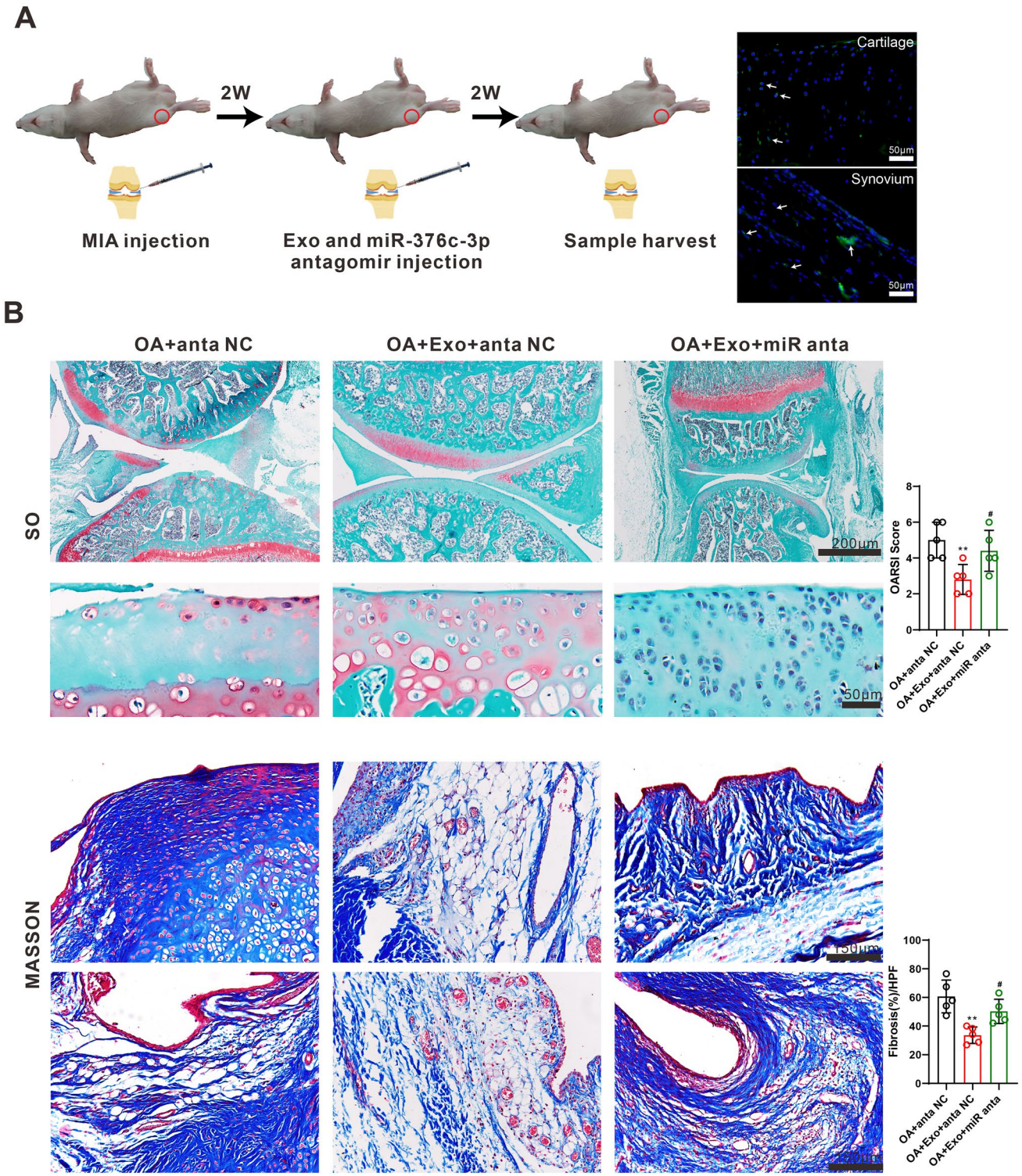

Fig. 6 miR-376c-3p in hADSC-derived Exos is involved in process of hADSC-derived Exos mitigating OA in rats. **A** The specific protocols for a rat model of OA and hADSC-derived Exos + miR-376c-3p antagomir injection. **B** SO Staining (Scale bar: 200 μm or 50 μm) and Masson staining (Scale bar: 150 μm) were applied to evaluate the degree of cartilage tissue degradation and synovial fibrosis. One-way ANOVA analysis combined with LSD post-hoc, N = 5. $^{**}P < 0.01$ versus OA + anta NC. $^{\#}P < 0.05$ versus OA + Exo + anta NC. Anta: antagomir

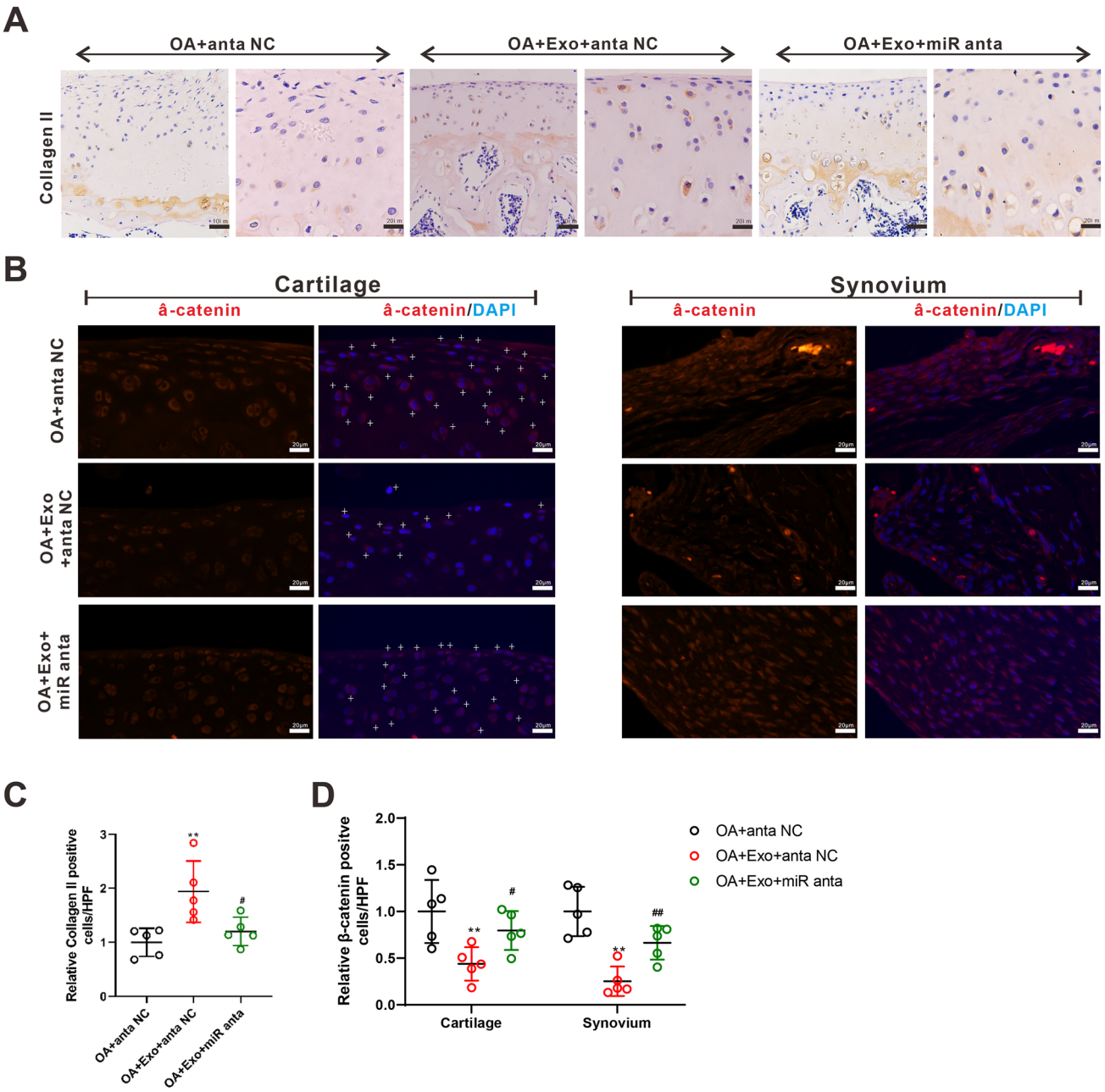

Fig. 7 Analysis of miR-376c-3p in hADSC-derived Exos on Collagen II and β-catenin in OA rats. **A** Immunohistochemical assay of Collagen II expression (Scale bar: 10 μm or 20 μm). **B** Immunofluorescence analysis of β-catenin expression (Scale bar: 20 μm). **C**, **D** Semi-quantitative statistical results of the above immunohistochemistry and immunofluorescence. One-way ANOVA analysis with LSD post-hoc. $^{**}P<0.01$ versus OA + anta NC. $^{\#}P<0.05$, $^{\#\#}P<0.01$ versus OA + Exo + anta NC

are more stable under different physiological conditions and present low immunogenicity [18]. Thus, the application of MSCs-derived Exos is more extensive.

In recent decades of research, it is generally believed that microRNAs (miRNAs) regulate the expressions of target genes at the post-transcriptional level by restraining the translation of mRNA or boosting mRNA degradation, thereby regulating various cellular processes [43, 44]. However, the instability of miRNAs in the extracellular environment severely restricts their functions. Increasing evidence expounds that Exos have the function of protecting miRNAs from degradation and miRNAs carried in

Exos can be applied as a pivotal means of communication between different cells [45, 46]. Recent studies authenticate that the miR-92a-3p in MSCs-derived Exos regulates cartilage development and maintains homeostasis by targeting WNT5a, hinting that exosomal miR-92a-3p has the potential to mitigate OA [33]. In the rat OA model, Exos derived from human synovial mesenchymal stem cells overexpressing miR-140-5p mitigate OA by strengthening cartilage tissues [47]. Here, we applied software available online (TargetScan) to computationally identify 19 miRNAs that might target the WNT-beta-catenin pathway-related important molecules WNT3 and WNT9a expressions both in rats and humans and discovered the sequences of 5 miRNAs were conserved in both rats and humans. Among these, we authenticated that miR-376c-3p was highly expressed in hADSC-derived Exos and miR-376c-3p targeted WNT3 and WNT9a. Importantly, miR-376c-3p, a conservative miRNA sequence, has been authenticate to mediate various cell apoptosis and injury [48], 49]. Our in-depth studies expounded that the miR-376c-3p in hADSC-derived Exos mitigated OA-induced chondrocyte degradation and synovial fibrosis both in vivo and in vitro.

Conclusion

In summary, our data authenticated that the novel and critically important miR-376c-3p in hADSC-derived Exos restrained the WNT-beta-catenin pathway by targeting WNT3/WNT9a, thereby mitigating OA-induced chondrocyte degradation and synovial fibrosis. Our experimental data confirmed that the miR-376c-3p in hADSC-derived Exos had the potential to mitigate OA, which might provide novel insights for the prevention and treatment of OA. Besides, the main limitation is that our research is still in the stage of basic research and has not been applied in clinical treatment.

Supplementary Information The online version contains supplementary material available at https://doi.org/10.1007/s10495-022-01787-0.

Acknowledgements Not applicable.

Author contributions FL, JX and GP contributed to the conception of the study and wrote the paper; ZX, ZX and XS contributed significantly to analysis and manuscript preparation; CL and YC participated in the design of the study. All authors read and approved the final manuscript.

Funding This study is supported by grants from the National Natural Science Foundation of China (No. 81802164).

Data availability All data generated or analyzed during this study are included in this published article.

Declarations

Competing interest All authors declare that they have no conflict of interest.

Ethical approval This study was approved by the Institute Research Medical Ethics Committee of the First Affiliated Hospital of Zhengzhou University.

Consent for publication Not applicable.

Research involving in human and animal participants This article contained studies with human adipose tissues for hADSCs isolation, in accordance with all principles of the Declaration of Helsinki, and the written informed consent was obtained from each participant. Rats were used for in vivo OA model establishment, and all animal experiments were conducted according to the AAALAC (Association for Assessment and Accreditation of Laboratory Animal Care) and the IACUC (Institutional Animal Care and Use Committee) guidelines.

References

1. Chen D, Shen J, Zhao W, Wang T, Han L, Hamilton JL, Im HJ (2017) Osteoarthritis: toward a comprehensive understanding of pathological mechanism. Bone Res 5:16044
2. Loeser RF, Goldring SR, Scanzello CR, Goldring MB (2012) Osteoarthritis: a disease of the joint as an organ. Arthritis Rheum 64(6):1697–1707
3. Reesink HL, Sutton RM, Shurer CR, Peterson RP, Tan JS, Su J, Paszek MJ, Nixon AJ (2017) Galectin-1 and galectin-3 expression in equine mesenchymal stromal cells (MSCs), synovial fibroblasts and chondrocytes, and the effect of inflammation on MSC motility. Stem Cell Res Ther 8(1):243
4. Steenvoorden MM, Bank RA, Ronday HK, Toes RE, Huizinga TW, DeGroot J (2007) Fibroblast-like synoviocyte-chondrocyte interaction in cartilage degradation. Clin Exp Rheumatol 25(2):239–245
5. Fosang AJ, Rogerson FM, East CJ, Stanton H (2008) ADAMTS-5: the story so far. Eur Cell Mater 15:11–26
6. Lee AS, Ellman MB, Yan D, Kroin JS, Cole BJ, van Wijnen AJ, Im HJ (2013) A current review of molecular mechanisms regarding osteoarthritis and pain. Gene 527(2):440–447
7. Remst DF, Blaney Davidson EN, van der Kraan PM (2015) Unravelling osteoarthritis-related synovial fibrosis: a step closer to solving joint stiffness. Rheumatol (Oxford) 54(11):1954–1963
8. Chang X, Shen J, Yang H, Xu Y, Gao W, Wang J, Zhang H, He S (2016) Upregulated expression of CCR3 in osteoarthritis and CCR3 mediated activation of fibroblast-like synoviocytes. Cytokine 77:211–219
9. Gupta A, Niger C, Buo AM, Eidelman ER, Chen RJ, Stains JP (2014) Connexin43 enhances the expression of osteoarthritis-associated genes in synovial fibroblasts in culture. BMC Musculoskelet Disord 15:425
10. Johnson K, Zhu S, Tremblay MS, Payette JN, Wang J, Bouchez LC, Meeusen S, Althage A, Cho CY, Wu X, Schultz PG (2012) A stem cell-based approach to cartilage repair. Science 336(6082):717–721
11. Vinatier C, Guicheux J (2016) Cartilage tissue engineering: from biomaterials and stem cells to osteoarthritis treatments. Ann Phys Rehabil Med 59(3):139–144

12. Mamidi MK, Das AK, Zakaria Z, Bhonde R (2016) Mesenchymal stromal cells for cartilage repair in osteoarthritis. Osteoarthr Cartil 24(8):1307–1316
13. ter Huurne M, Schelbergen R, Blattes R, Blom A, de Munter W, Grevers LC, Jeanson J, Noël D, Casteilla L, Jorgensen C, van den Berg W, van Lent PL (2012) Antiinflammatory and chondroprotective effects of intraarticular injection of adipose-derived stem cells in experimental osteoarthritis. Arthritis Rheum 64(11):3604–3613
14. Zhang R, Ma J, Han J, Zhang W, Ma J (2019) Mesenchymal stem cell related therapies for cartilage lesions and osteoarthritis. Am J Trans Res 11(10):6275–6289
15. Herberts CA, Kwa MS, Hermsen HP (2011) Risk factors in the development of stem cell therapy. J Transl Med 9:29
16. Kourembanas S (2015) Exosomes: vehicles of intercellular signaling, biomarkers, and vectors of cell therapy. Annu Rev Physiol 77:13–27
17. Théry C, Ostrowski M, Segura E (2009) Membrane vesicles as conveyors of immune responses. Nat Rev Immunol 9(8):581–593
18. Chang YH, Wu KC, Harn HJ, Lin SZ, Ding DC (2018) Exosomes and stem cells in degenerative disease diagnosis and therapy. Cell Transplant 27(3):349–363
19. Xin H, Li Y, Chopp M (2014) Exosomes/miRNAs as mediating cell-based therapy of stroke. Front Cell Neurosci 8:377
20. Zhu Y, Wang Y, Zhao B, Niu X, Hu B, Li Q, Zhang J, Ding J, Chen Y, Wang Y (2017) Comparison of exosomes secreted by induced pluripotent stem cell-derived mesenchymal stem cells and synovial membrane-derived mesenchymal stem cells for the treatment of osteoarthritis. Stem Cell Res Ther 8(1):64
21. Hong P, Yang H, Wu Y, Li K, Tang Z (2019) The functions and clinical application potential of exosomes derived from adipose mesenchymal stem cells: a comprehensive review. Stem Cell Res Ther 10(1):242
22. Guo J, Hu H, Gorecka J, Bai H, He H, Assi R, Isaji T, Wang T, Setia O, Lopes L, Gu Y, Dardik A (2018) Adipose-derived mesenchymal stem cells accelerate diabetic wound healing in a similar fashion as bone marrow-derived cells. Am J Physiol Cell Physiol 315(6):C885-c896
23. Liu X, Zhu W, Wang L, Wu J, Ding F, Song Y (2019) miR-145–5p suppresses osteogenic differentiation of adipose-derived stem cells by targeting semaphorin 3A. In vitro cellular and developmental biology. Animal 55(3):189–202
24. Deng S, Zhou X, Ge Z, Song Y, Wang H, Liu X, Zhang D (2019) Exosomes from adipose-derived mesenchymal stem cells ameliorate cardiac damage after myocardial infarction by activating S1P/SK1/S1PR1 signaling and promoting macrophage M2 polarization. Int J Biochem Cell Biol 114:105564
25. Philpott HT, McDougall JJ (2020) Combatting joint pain and inflammation by dual inhibition of monoacylglycerol lipase and cyclooxygenase-2 in a rat model of osteoarthritis. Arthritis Res Ther 22(1):9
26. He L, He T, Xing J, Zhou Q, Fan L, Liu C, Chen Y, Wu D, Tian Z, Liu B, Rong L (2020) Bone marrow mesenchymal stem cell-derived exosomes protect cartilage damage and relieve knee osteoarthritis pain in a rat model of osteoarthritis. Stem Cell Res Ther 11(1):276
27. Ko JY, Lee MS, Lian WS, Weng WT, Sun YC, Chen YS, Wang FS (2017) MicroRNA-29a counteracts synovitis in knee osteoarthritis pathogenesis by targeting VEGF. Sci Rep 7(1):3584
28. Fang S, Xu C, Zhang Y, Xue C, Yang C, Bi H, Qian X, Wu M, Ji K, Zhao Y, Wang Y, Liu H, Xing X (2016) Umbilical cord-derived mesenchymal stem cell-derived exosomal MicroRNAs suppress myofibroblast differentiation by inhibiting the transforming growth factor-β/SMAD2 pathway during wound healing. Stem Cells Transl Med 5(10):1425–1439
29. Chapel DB, Schulte JJ, Husain AN, Krausz T (2020) Application of immunohistochemistry in diagnosis and management of malignant mesothelioma. Trans Lung Cancer Res 9(Suppl 1):S3-s27
30. Li L, Li M, Pang Y, Wang J, Wan Y, Zhu C, Yin Z (2019) Abnormal thyroid hormone receptor signaling in osteoarthritic osteoblasts regulates microangiogenesis in subchondral bone. Life Sci 239:116975
31. Flomerfelt FA, Gress RE (2016) Analysis of cell proliferation and homeostasis using EdU labeling. Methods Mol Biol 1323:211–220
32. Wang L, Yang J, Wang H, Wang W, Liang X (2020) Highly expressed ribosomal protein L34 predicts poor prognosis in acute myeloid leukemia and could be a potential therapy target. Aging Pathobiol Ther 2(1):32–37
33. Mao G, Zhang Z, Hu S, Zhang Z, Chang Z, Huang Z, Liao W, Kang Y (2018) Exosomes derived from miR-92a-3p-overexpressing human mesenchymal stem cells enhance chondrogenesis and suppress cartilage degradation via targeting WNT5A. Stem Cell Res Ther 9(1):247
34. Niu Y, Zhou B, Wan C et al (2020) Down-regulation of miR-181a promotes microglial M1 polarization through increasing expression of NDRG. Aging Pathobiol Ther 2(1):52–57
35. Kimura K, Hohjoh H, Fukuoka M, Sato W, Oki S, Tomi C, Yamaguchi H, Kondo T, Takahashi R, Yamamura T (2018) Circulating exosomes suppress the induction of regulatory T cells via let-7i in multiple sclerosis. Nat Commun 9(1):17
36. Lietman C, Wu B, Lechner S, Shinar A, Sehgal M, Rossomacha E, Datta P, Sharma A, Gandhi R, Kapoor M, Young PP (2018) Inhibition of Wnt/β-catenin signaling ameliorates osteoarthritis in a murine model of experimental osteoarthritis. JCI insight. https://doi.org/10.1172/jci.insight.96308
37. Johnsen KB, Gudbergsson JM, Skov MN, Pilgaard L, Moos T, Duroux M (2014) A comprehensive overview of exosomes as drug delivery vehicles - endogenous nanocarriers for targeted cancer therapy. Biochem Biophys Acta 1846(1):75–87
38. Rani S, Ryan AE, Griffin MD, Ritter T (2015) Mesenchymal stem cell-derived extracellular vesicles: toward cell-free therapeutic applications. Mol Ther 23(5):812–823
39. Yeo RW, Lai RC, Zhang B, Tan SS, Yin Y, Teh BJ, Lim SK (2013) Mesenchymal stem cell: an efficient mass producer of exosomes for drug delivery. Adv Drug Deliv Rev 65(3):336–341
40. Zhou Y, Wang T, Hamilton JL, Chen D (2017) Wnt/β-catenin signaling in osteoarthritis and in other forms of arthritis. Curr Rheumatol Rep 19(9):53
41. Deshmukh V, O'Green AL, Bossard C, Seo T, Lamangan L, Ibanez M, Ghias A, Lai C, Do L, Cho S, Cahiwat J, Chiu K, Pedraza M, Anderson S, Harris R, Dellamary L, Kc S, Barroga C, Melchior B, Tam B, Kennedy S, Tambiah J, Hood J, Yazici Y (2019) Modulation of the Wnt pathway through inhibition of CLK2 and DYRK1A by lorecivivint as a novel, potentially disease-modifying approach for knee osteoarthritis treatment. Osteoarthr Cartil 27(9):1347–1360
42. Yazici Y, McAlindon TE, Fleischmann R, Gibofsky A, Lane NE, Kivitz AJ, Skrepnik N, Armas E, Swearingen CJ, DiFrancesco A, Tambiah JRS, Hood J, Hochberg MC (2017) A novel Wnt pathway inhibitor, SM04690, for the treatment of moderate to severe osteoarthritis of the knee: results of a 24-week, randomized, controlled, phase 1 study. Osteoarthr Cartil 25(10):1598–1606
43. Chen L, Heikkinen L, Wang C, Yang Y, Sun H, Wong G (2019) Trends in the development of miRNA bioinformatics tools. Brief Bioinform 20(5):1836–1852
44. Correia de Sousa M, Gjorgjieva M, Dolicka D, Sobolewski C, Foti M (2019) Deciphering miRNAs' action through miRNA editing. Int J Mol Sci 20(24):6249

45. Mayourian J, Ceholski DK, Gorski PA, Mathiyalagan P, Murphy JF, Salazar SI, Stillitano F, Hare JM, Sahoo S, Hajjar RJ, Costa KD (2018) Exosomal microRNA-21-5p mediates mesenchymal stem cell paracrine effects on human cardiac tissue contractility. Circ Res 122(7):933–944
46. Wang R, Xu B, Xu H (2018) TGF-β1 promoted chondrocyte proliferation by regulating Sp1 through MSC-exosomes derived miR-135b. Cell Cycle 17(24):2756–2765
47. Tao SC, Yuan T, Zhang YL, Yin WJ, Guo SC, Zhang CQ (2017) Exosomes derived from miR-140-5p-overexpressing human synovial mesenchymal stem cells enhance cartilage tissue regeneration and prevent osteoarthritis of the knee in a rat model. Theranostics 7(1):180–195
48. Wang K, Jin J, Ma T, Zhai H (2017) MiR-376c-3p regulates the proliferation, invasion, migration, cell cycle and apoptosis of human oral squamous cancer cells by suppressing HOXB7. Biomed Pharmacother 91:517–525
49. Zhang H, Zhou J, Zhang M, Yi Y, He B (2019) Upregulation of miR-376c-3p alleviates oxygen-glucose deprivation-induced cell injury by targeting ING5. Cell Mol Biol Lett 24:67